International Journal of Advanced Science and Technology
Vol.116 (2018), pp.131-140
http://dx.doi.org/10.14257/ijast.2018.116.12

Adaptive Filtering for Attitude Estimation System in Harsh Vibration Environment

Sang Cheol Lee and Sung Kyung Hong*

Department of Aerospace Engineering, Sejong University, Korea
tend00@sju.ac.kr, skhong@sejong.ac.kr

Abstract

This paper presents the adaptive algorithm for a low-cost and low-weight attitude estimation system of the light aircraft using a MEMS (Micro-Electro-Mechanical System) inertial sensor. The proposed approach relies on two parts: 1) Pre-processing of accelerometer sensor data measured in harsh environment such as strong vibration. This approach utilizes sinusoidal estimation to continuously adapt the filtering bandwidth of the accelerometer's data in order to reduce the effects of vibration and sensor noise before attitude estimation is processed 2) Design of adaptive complementary filter for an aiding system using accelerometer and gyro sensor. This approach relies on a gain-scheduled complementary filter, augmented by an angular rate-based switching architecture. The cut-off frequency of the filter is determined adaptively under varying light aircraft dynamics. The proposed method is applied to light aircraft and the experimental data demonstrate the effectiveness of this approach.

Keywords: *MEMS IMU; Aiding system; Harsh environment*

1. Introduction

Cost effective MEMS (Micro-Electro-Mechanical Systems)-based sensors are being used more than ever for deriving navigation information on a light aircraft and drones. A strapdown inertial navigation system consists of 3-axis accelerometers and gyros and is mainly used to estimate the attitude, velocity, and position of an aircraft [1–3]. MEMS sensors, which are relatively small and light, can provide navigation solutions at low cost. Usually, an aircraft's attitude can be obtained by integrating rotational angular velocities measured by a gyro sensor. However, a MEMS-based inertial sensor generates unbounded errors owing to such factors as relatively large bias instability, insufficient sensitivity, and noise. This problem can be diminished by building an aiding system using accelerometers. However, such an MEMS-based aiding system cannot produce an ideal result in a harsh environment (*e.g.*, engine vibrations) [4]. This study focuses on the pre-processing filter design for effectively removing vibration and sensor noise and presents a robust aiding system design for estimating attitude in a dynamic environment.

It is not easy to decrease only the impact of vibration in a complex signal that mixes the impact of vibration and the dynamics of an aircraft. Because an accelerometer usually measures translational acceleration, centrifugal force, and gravitational acceleration, it is affected by vibrations generated by the propeller and the aircraft's body. Further, a gyro measuring rotational angular velocity is less affected by vibrations. A harsh environment has a direct effect on an accelerometer such that attitude accuracy can decline, so an aiding system is necessary. Because acceleration data need to be as minimally affected as possible by vibration or other effects of the external environment to estimate attitude accurately, pre-processing of an accelerometer is essential. The pre-processing algorithm proposed in this study was designed to adjust filtering frequency adaptively based on signal history to

Received (November 26, 2017), Review Result (February 15, 2018), Accepted (March 10, 2018)

ISSN: 2005-4238 IJAST

provide effective filtering. Acceleration signals with reduced vibration components were used to configure a gyro and an aiding system, thereby improving attitude estimation.

Because low frequency components of a gyro usually cause an unbounded error, the reliability of a gyro is higher in a dynamic condition (*i.e.*, during aircraft maneuvers) than in a static condition. However, an accelerometer can be effectively used for attitude estimation in an aiding system when a gravity component is the main measurement factor in a static condition [5–8]. This is because the curved path of an aircraft flying in a level circle generates additional acceleration that is not necessary for an attitude estimation. An appropriate aiding system design using this difference in characteristics can produce highly accurate attitude estimations. The proposed aiding system includes a simple fusion filter to estimate attitude accurately in various dynamic situations [9 – 10]. Robust attitude estimation is possible by using angles to identify dynamic conditions and modifying the corresponding gains of the fusion filter.

2. Pre-Processing Design

In a harsh environment, as accelerometers are directly affected by structural vibration or by strong vibration of a propeller, the attitude accuracy may be degraded when an aiding system is first configured. Because acceleration data need to be as minimally affected as possible by vibration or external factors to estimate attitude accurately, pre-processing of an accelerometer is essential.

2.1. Flight Characteristics of the Test Aircraft

The test aircraft used is classified as being in the Level 1, Class 1, and Category B flight phase by the Federal Aviation Administration (FAA). Table 1 presents detailed specifications. The time required for bank or pitch angle changes is defined to be between 0.2 s and 1.7 s, which means that the operational frequency of an aircraft ranges between 0.6 Hz and 5 Hz [11]. Once the operational frequency of an aircraft is known, an ideal band pass filter (BPF) could be designed. However, such a filter (with narrow bandwidth) is not suitable because it requires a high order frequency and generates a time delay. As mentioned above, the dynamic frequency of the light aircraft changes between 0.6 Hz and 5 Hz. For this reason, a Kaiser Window BPF was used for effective pre-processing. For each flight condition, the main dynamic frequency was estimated, and the cutoff frequency was modified, thereby removing components other than the dynamic frequency effectively.

2.2. Sinusoidal Wave Estimation

Figure 1 shows the overall block diagram for estimating the main dynamic frequency according to flight conditions. After data collection (~1 s), the dynamic frequency is estimated by sinusoidal wave estimation. If N data (x_n) are input into a sensor at time t_n, this can be expressed by (1). If the signal is assumed to be a sinusoidal wave, it can be expressed by (2) [12].

$$x_n = [x_1, x_2, \dots x_{N-1}, x_n]^T; t_n = [t_1, t_2 \dots t_{N-1}, t_N] \quad (1)$$

$$x_n = Acos(\omega \times t_n) + Bsin(\omega \times t_n) + C \quad (2)$$

Table 1. Specification-Flying Qualities of a Light Aircraft

Classification of Airplanes	
Class 1	Small, light airplanes such as, Light utility, Primary trainer, Light observation
Flight Phase Categories	
Category B	a. Climb (CL), b. Cruise (CR), c. Loiter (LO) d. In-flight refueling (tanker) (RT), e. Descent(D), f. Emergency descent (ED), g. Emergency deceleration (DE) h. Aerial delivery (AD).
Levels of Flying Qualities	
Level 1	Flying qualities clearly adequate for the mission Flight Phase

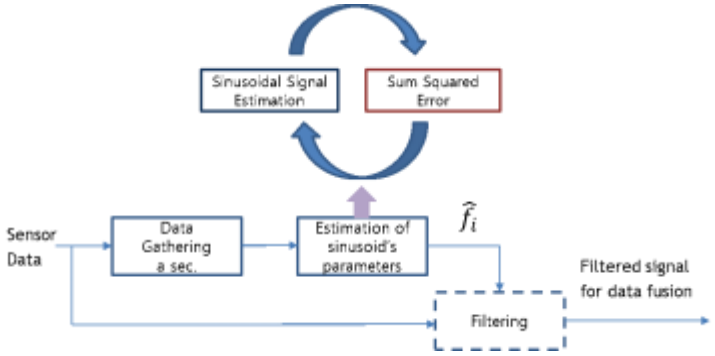

Figure 1. Dynamic Frequency Estimation Block Diagram

In the two formulas, A and B are amplitudes of signals, C is the bias, ω is the frequency of signal. $D(\omega)$, and θ can be defined as in (3) and (4) below.

$$\theta = [A\ B\ C]^T \tag{3}$$

$$D(\omega) = \begin{bmatrix} \cos(\omega \times t_1) & \sin(\omega \times t_1) & 1 \\ \vdots & \vdots & \vdots \\ \cos(\omega \times t_N) & \sin(\omega \times t_N) & 1 \end{bmatrix} \tag{4}$$

Formula (2) can be simplified into the following formula using (3) and (4).

$$x_n = D(\omega)\theta \tag{5}$$

Here, the least squares method is applied to derive the coefficients $\hat{\theta}$ that determine the characteristics of a signal. The estimation can be expressed as follows.

$$\hat{\theta} = \begin{pmatrix} \hat{A} \\ \hat{B} \\ \hat{C} \end{pmatrix} = (D(\omega)^T D(\omega))^{-1} D(\omega)^T x_n \tag{6}$$

If ω is known in (6), the characteristics of a current input signal can be identified by estimating $\hat{\theta}$. However, ω cannot be known, so an original signal can be estimated by creating an arbitrary signal as defined by (7).

$$\hat{x}_n = \hat{A}cos(2\pi\hat{f}_i \times t_n) + \hat{B}sin(\omega \times t_n 2\pi\hat{f}_i \times t_n) + \hat{C} \tag{7}$$

Formula (7) is used to add a margin to the starting frequency ($\hat{f}_i$) of the light aircraft, and thus, an arbitrary signal ($\hat{x}_n$) can be generated by inputs from 0.2 Hz to 7 Hz. When the integrated squared error between an estimated signal ($\hat{x}_n$) and an original signal (x_n) is lowest based on the sum squared error, (8), the original signal

is similar to an arbitrarily created signal. In other words, for a currently input signal ($\hat{f}_i$), $\widehat{f_i} \approx f_i$ can be valid and the dynamic frequency of the original signal can be estimated.

$$SSE = \sum_1^N (x_n - \hat{x}_n)^2 \tag{8}$$

2.3. Kaiser Window Filter

A Kaiser window filter, which can adequately adjust the transition band and pass/stop band ripples, was designed as the pre-processing filter. The weighting coefficients $h(n)$ of the Kaiser window filter are calculated by (9), which consists of a Kaiser window function(n) and an impulse response function $h_{BP}(n)$, which is a form of a band pass filter.

$$h(n) = \omega(n) h_{BP}(n) \tag{9}$$

Figure 2 shows the overall block diagram of the Kaiser window filter. The Kaiser window function in (9) can be defined as (10) below.

$$\omega(n) = \frac{I_0\left(\sqrt{\left(1-\left(\frac{n-M/2}{M/2}\right)^2\right)}\right)}{I_0(\beta)} \tag{10}$$

In (10), I_0 is a Bessel function, and β is a positive real number coefficient determining the shape of the Kaiser window. M is the order of the filter. The Bessel function (I_0) can be expressed by (11).

$$I_0(x) = 1 + \sum_{k=0}^{\infty} \left(\frac{(x/2)^k}{k!}\right)^2 \tag{11}$$

In addition, β (that defines the shape of the Kaiser window) in (10) can be presented as follows.

$$\beta = \begin{cases} 0.1102(A - 8.7) & A \geq 50 \\ 0.5842(A-21)^{0.4} + 0.007886(A-21) & 21 < A \leq 50 \\ 0 & A \leq 21 \end{cases} \tag{12}$$

The relationship between A and the ripple can be expressed by (13) below.

$$A = -20\, log_{10}(ripple) \tag{13}$$

The order of the filter in (10) is calculated from (14).

$$M + 1 = \begin{cases} \frac{A-7.95}{2.285\Delta\omega} & A > 21 \\ \frac{5.79}{\Delta\omega} & A \leq 21 \end{cases} \tag{14}$$

Above, β is a non-negative real number and determines the Kaiser window shape, as shown in Figure 3. In the frequency domain, the main-lobe width and the side-lobe level can be determined. The bandwidth decreases with increasing side-lobe. The impulse response function h_{BP} has a band pass filter (BPF) shape and can be expressed by (15).

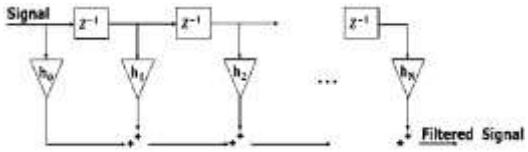

Figure 2. Block Diagram of the Kaiser Window Filter

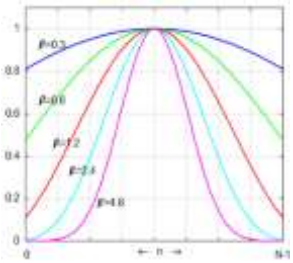

Figure 3. Kaiser Window Shape

The BPF can be set by using a dynamic frequency ($\hat{f}_i$) previously estimated and by setting the corresponding bandwidth.

$$h_{BP}(n) = \begin{cases} \frac{sin(\omega_{C2}(2n/M-1)}{\pi(2n/M-1)} & ,0 < n < M, n \neq \frac{M}{2} \\ \frac{\omega_{c2}}{\pi} - \frac{\omega_{c1}}{\pi} & ,n = \frac{M}{2} \end{cases} \quad (15)$$

Figure 4 illustrates the simulation results of pre-processing. The upper graph shows the final denoised result and the lower displays the corresponding estimations of the dynamic frequency. In the simulation, 3 Hz, 2 Hz and 1 Hz sinusoidal signals (green solid line) were generated at 3-s intervals. White noise of approximately $0.0135°/\text{sec}/\sqrt{Hz}$ was applied to the reference signal generated to create a signal similar to that of a real sensor (blue solid line). The red dotted line is the final pre-processing result of the signal to which the noise was applied. As shown in the estimations of dynamic frequency below, the frequency of an applied signal was accurately estimated after the initial 0.5 s after each frequency was applied. As the initial data gathering at each frequency used a previously estimated frequency for filter application, some noise was observed initially. However, after a frequency was accurately estimated, such noise was removed from the main dynamic frequency. In other words, each dynamic frequency was effectively filtered.

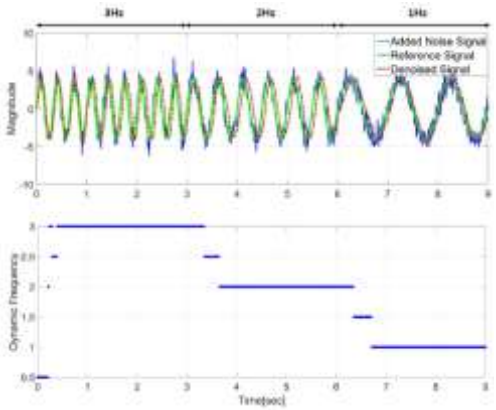

Figure 4. Pre-processing Result (upper), Result of Estimations of Dynamic Frequency (lower)

3. Aiding System Design

3.1. Attitude Estimation using an Inertial Sensor

Both a gyro and an accelerometer can estimate an aircraft's attitude. The gyro measures rotational angular velocities and integrates them to estimate attitude. However, because the strapdown gyro measures the body-axis angular velocity, it requires a preliminary coordinate transformation. The relationship between gyro measurements (p, q, r) and the temporal rate of Euler angles $(\dot{\phi}, \dot{\theta}, \dot{\psi})$ can be expressed by a direction cosine matrix, as shown in (16).

$$\begin{bmatrix} \dot{\phi} \\ \dot{\theta} \\ \dot{\psi} \end{bmatrix} = \begin{bmatrix} 1 & sin\phi tan\theta & cos\phi tan \\ 0 & cos\phi & -sin\phi \\ 0 & sin\phi/cos\theta & cos\phi/cos\theta \end{bmatrix} \begin{bmatrix} p \\ q \\ r \end{bmatrix} \tag{16}$$

To estimate attitude using an accelerometer, a 6-DOF (degree of freedom) equation of motion is defined as follows.

$$f = \begin{bmatrix} \dot{u}_b \\ \dot{v}_b \\ \dot{w}_b \end{bmatrix} = \begin{bmatrix} 0 & w_b & -v_b \\ -w_b & 0 & -sin\phi \\ v_b & -u_b & 0 \end{bmatrix} \begin{bmatrix} p \\ q \\ r \end{bmatrix} + g \begin{bmatrix} sin\theta \\ -cos\theta sin\phi \\ -cos\theta cos\phi \end{bmatrix} \tag{17}$$

In (17), f is the acceleration value, $\dot{u}_b, \dot{v}_b, \dot{w}_b$ are the accelerations of the real motions of the body-axis, u_b, v_b, w_b are the velocities measured at the body-axis, p, q, r are rotational angular velocities, and g is the gravitational acceleration of the earth. If a static condition is assumed, where only the effect of gravitational acceleration of the earth exists, the following formula applies.

$$f = \begin{bmatrix} f_x \\ f_y \\ f_z \end{bmatrix} \approx \begin{bmatrix} sin\theta \\ -cos\theta sin\phi \\ -cos\theta cos\phi \end{bmatrix} \tag{18}$$

In (18), f_x, f_y, f_z are measurements by an accelerometer. The following formula then describes the attitude.

$$\phi_a = tan2^{-1}\left(\frac{f_y}{f_z}\right), \theta_a = tan2^{-1}\left(\frac{-f_x}{\sqrt{f_y^2 + f_z^2}}\right) \tag{19}$$

3.2. Adaptive Complementary Filter Design

The gyro has reliable high frequency responses but its low frequency responses are much less reliable, as they cause unbounded divergence. However, in the case of an accelerometer, high frequency responses are not reliable while low frequency ones are very reliable. The signals with such opposite frequency responses can be combined by applying a complementary filter to improve overall performance. Figure 5 shows the block diagram of an adaptive complementary filter. Unlike conventional complementary filters, the adaptive complementary filter can change its cutoff frequency to accurately estimate the attitude in various dynamic situations. This is explained by means of roll (pitch can also demonstrate the same). Assume that $\dot{\phi}_g$ is the temporal rate of Euler angles, which was converted from the gyro measurement, ϕ_a is the attitude value estimated by (19) for the accelerometer measurement, $\dot{\phi}_b$ is the estimated bias drift value of the gyro, and ϕ_m is the

result of the attitude estimation. Then formula (20) expresses the complementary filter in Laplace form.

$$\phi_m = \frac{1}{s}\dot{\phi}_g + \frac{K_p}{s}(\phi_a - \phi_m) + \frac{K_i}{S^2}(\phi_a - \phi_m) \tag{20}$$

$$\phi_m = \frac{s^2}{s^2 K_p s + K_i}\frac{\dot{\phi}_g}{s} + \frac{K_p s + K_i}{s^2 K_p s + K_i}\phi_a \tag{21}$$

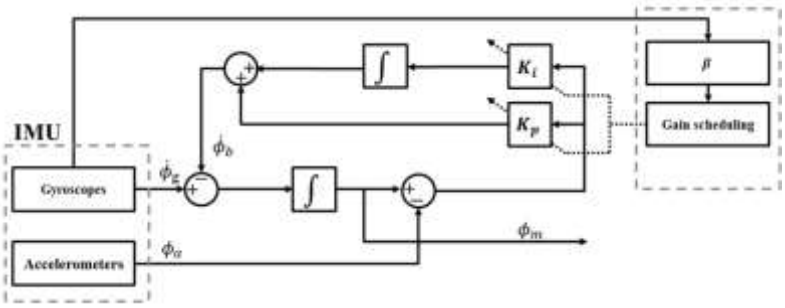

Figure 5. Adaptive Complementary Filter Block Diagram

K_i and K_p are determined by setting the cutoff frequency (ω) and the damping ratio(ζ), as shown in (22).

$$K_i = \omega^2, K_p = 2\zeta\omega \tag{22}$$

In this case, the damping ratio(ζ) was set to 0.707 to reflect transient responses, and K_p was obtained from (23).

$$K_p = \sqrt{2}\omega \tag{23}$$

The characteristics of a complementary filter depend on a cutoff frequency. An optimal complementary filter can be designed by adjusting the weights of two signals and thus setting an adequate cutoff frequency. The cutoff frequency is defined by combining high and low pass filters. Accelerometers use the low pass filter, while gyros use the high pass filter. As shown in (22) and (23), a complementary filter is designed by defining the desired cutoff frequency. This cutoff frequency can be modified according to dynamic conditions. Formula (24) is the criterion for determining which dynamic condition applies. In the formula, p, q, r are gyro measurements, and a dynamic condition is identified through calculation of $\beta(k)$. Table 2 presents the gain variation according to dynamic conditions. A 3-level scheme (High, Middle, Low) was applied to each parameter. Every gain value was experimentally determined.

$$\beta(k) = \left|\sqrt{p^2 + q^2 + r^2}\right| \tag{24}$$

Table 2. Parameters for Dynamic Conditions

Parameter	High	Middle	Low
Beta $\boldsymbol{\beta(k)}$	$\beta(k) \geq 15$	$5 < \beta(k) < 15$	$\beta(k) \leq 5$
Cut-off Frequency $\boldsymbol{\omega(k)}$	0.009	$\omega(k) = -0.002\beta + 0.04$	0.03

4. Light Aircraft Flight Test

As shown in Figure 6 (left), an attitude reference system (ARS) was designed to verify the proposed algorithm. The ARS was composed of an IMU (Inertial Measurement Unit) and DSP (Digital Signal Processor). The IMU was an Analog Device ADIS 16488 [13]. The device consists of 3-axis gyros and 3-axis accelerometers, and provides the acceleration and rotational angular velocity of the body frame. The DSP used was a Texas Instruments TMS320 F28335. The estimation results were derived by applying the designed algorithm. The aircraft used for flight tests was Flight Design's (Germany) CTLS model. As shown in Fig. 6 (right), it was a two-seater light aircraft owned by KARI (Korea Aerospace Research Institute). For comparison with a reference, a commercial NAV440 inertial navigation system manufactured by Crossbow was installed in the CTLS along with the designed attitude reference system.

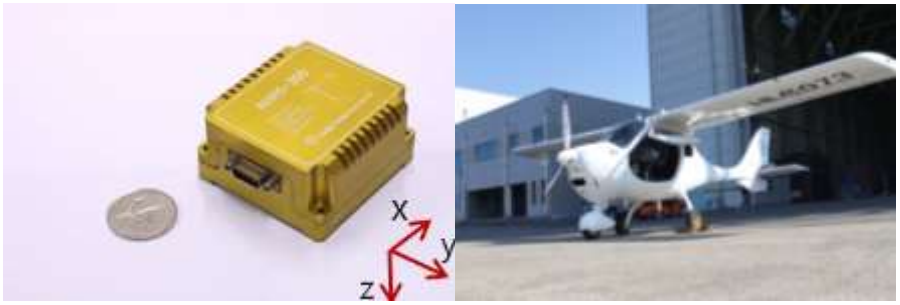

Figure 7. Attitude Reference System (left), Light Aircraft for Flight Test (right)

The flight test was conducted for the following profile: Take-off - Longitudinal Phugoid flight - Dutch roll flight - Bank 30 deg Circle flight - Bank - 30 deg Circle flight - Landing. Figure 7(left) shows the comparison between raw data of acceleration measured during the entire flight and data after pre-processing. Figure 7 (right) depicts the measurements of the Y-axis acceleration during the Dutch roll flight and the corresponding estimations of dynamic frequency. From the results, adequate estimations of input frequency resulted in good filtering.

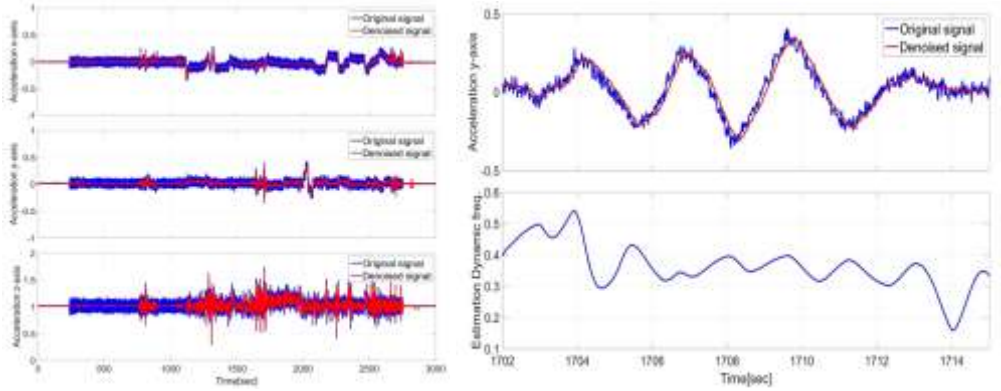

Figure 7. Acceleration Measurement Data during the Flight Test (left), Y-axis Acceleration Measurements during Dutch roll flight [1702-1715 sec] and Estimations of Dynamic Frequency (right)

The red solid line of Figure 11 is the result of combining the pre-processed accelerometer signals and the gyro signals. The blue solid line is the reference (Crossbow NAV 440). Comparison with the reference shows that attitudes were accurately estimated.

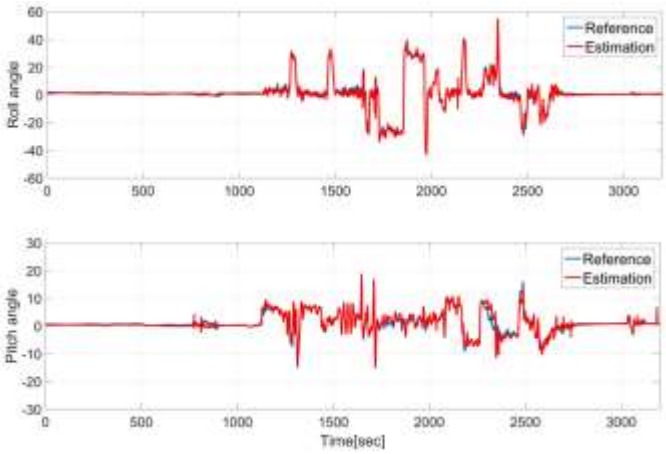

Figure 8. Attitude Estimations (roll, pitch)

5. Conclusion

This study has proposed a pre-processing filter design and an aiding system design achieved by using a MEMS-based inertial sensor in a harsh environment including a strong vibration, such as in a piloted aircraft. For pre-processing before attitude estimation, the dynamic frequency of an aircraft was estimated to remove noise components from the signals of an accelerometer that was relatively susceptible to vibration. Then, the design of a gain scheduled adaptive complementary filter provided an effective method of attitude estimation. The proposed method was verified by a flight test of a light aircraft, where the comparison with a commercial navigation system used as a reference was made.

Acknowledgments

This work was supported by the Korea Institute for Advencement of Technology(KIAT) grant funded by the Korean government (Motie: Ministry of Trade, Industry&Energy) (No. N0002431).

References

[1] R. Zhu, and Z. Zhou, "A Small Low-Cost Hybrid Orientation System and Its Error Analysis", IEEE Sensor Journal, vol. 9, no. 3, **(2009)** March, pp. 223-230.
[2] W. J. Fleming, "New Automotive Sensors. A Review", IEEE Sensors Journal, vol. 8, no. 11, **(2008)**, pp. 1900-1921.
[3] R. Neul, U.-M. Gomez, K. Kehr, W. Bauer, J. Classen, C. Doring, E. Esch, S. Gotz, J. Hauer, B. Kuhlmann, C. Lang, M. Veith and R. Willig, "Micromachined Angular Rate Sensors for Automotive Applications", IEEE Sensors Journal, vol. 7, no. 2, **(2007)**, pp. 302-309.
[4] R. Jan, R. Michal and D. Karel, "Data Processing of Inertial Sensors in Strong-Vibratio Environment", IEEE International Conference on Intelligent Dapa Acquisition, **(2011)** September 15-17.
[5] D. Gebre-Egziabher, R. C. Hayward and J. D. Powell, "Design of multisensory attitude determination systems", IEEE Transactions on Aerospace and Electronic System, vol. 40, **(2004)**, pp. 627-649.
[6] Y. S. Suh, S. K. Park and H. J. Kang, "Attitude estimation adaptively compensating external acceleration", JSME International Journal, vol. 49, no. 1, **(2006)**, pp. 172-179.
[7] T. S. Yoo, S. K. Hong, H. M. Yoon, "Gain-scheduled complementary filter design for a MEMS based attitude and heading reference system", Sensors, vol. 11, **(2011)**, pp. 3816-3830.
[8] H. Rehbindera and X. M. Hu, "Drift-free attitude estimation for accelerated rigid bodies", Automatica, vol. 40, **(2004)**, pp. 653.659.
[9] S. K. Hong, "Compensation of nonlinear thermal bias drift of Resonant Rate Sensor (RRS) using fuzzy logic", Sens. Actuat. A Phys., vol. 78, **(1999)**, pp. 143-148.
[10] S. K. Hong, "Minimal-Drift Heading Measurement using a MEMS Gyro for Mobile Robots: Fused with Odometry", International Journal of Control, Automation, and Systems, vol. 10, no. 5, **(2012)**, pp. 1-5.
[11] D. J. Moorhouse and R. J. Woodcock, "Background Information and User Guide for MIL-F-8785C, Military Specification-Flying Qualities of Piloted Airplanes", Air Force Wright Aeronautical Labs Wright-Patterson Air Force Base: Dayton, OH, USA, **(1982)**.

[12] IEEE Standard for Terminology and Test. Methods for Analog-To-Digital Converters, **(2001)**, pp. 1-92, Available online: http:// ieee xplore.ieee.org/stamp/ stamp.jsp arnumber= 929859
[13] Tri-Axis Inertial sensor, ADIS16488; Analog Devices: Norwood, MA, USA, **(2011)**.

Authors

Sang Cheol Lee, 2012 B.S. at the Department of Mechanical and Aerospace Engineering of Sejong University 2012- present Ph. D student in Mechanical and Aerospace Engineering at Sejong University Main interest: Integrated navigation algorithm, Sensor fusion, Embedded system.

Sung Kyung Hong, 1987 B.S. at the Department of Mechanical Engineering of Yonsei University. 1989 M.S. at the Graduate School of Mechanical Engineering of Yonsei University. 1998 Ph.D. in Engineering at Texas A&M Univ. 1989~2000 Senior researcher at the Agency of Defense Development 2000 ~ present Professor of the Department of Mechanical and Aerospace Engineering at Sejong University Main interest: Design of navigation guidance and control system.

